A DLM FOR T-TAILS

Louw H van Zyl

DPSS, CSIR
P O Box 395, Pretoria, 0001, South Africa
e-mail: lvzyl@csir.co.za

Keywords: Subsonic Unsteady Aerodynamics, Doublet Lattice Method, T-tail

Abstract. This paper describes the extension of the DLM to account for effects that are critical to the modelling of T-tail flutter. The boundary condition is made more general to account for yaw/dihedral and sideslip/dihedral coupling and the calculation of forces is generalised to account for lateral load due to roll, and rolling moment due to yaw, yaw rate and sideslip. In addition, the steady load and the quadratic components of the mode shapes are taken into account in the calculation of generalised forces.

NOMENCLATURE

C_p^0	steady pressure coefficient
C_p^1	unsteady pressure coefficient
$\underline{F} = \underline{F}_0 + \underline{F}_1 e^{i\omega t}$	total force vector
$\underline{F}_0$	steady force vector
$\underline{F}_1 = \sum_{j=1}^{n} q_j \underline{F}_j$	total unsteady force vector
$\underline{F}_j$	unsteady force vector due to mode j
$\underline{h}$	modal displacement vector
$\underline{h}_i^1$	linear modal displacement due to mode i
$\underline{h}_i^2$	quadratic modal displacement due to mode i
k	reduced frequency,
$\underline{n} = \underline{n}_0 + \underline{r} e^{i\omega t} \times \underline{n}_0$	instantaneous normal vector
$\underline{n}_0$	mean normal vector in global coordinates
q_j	generalised coordinate j
$\underline{r}$	modal rotation vector
U	free stream velocity
$\underline{u} = \underline{u}_\infty + \underline{u}_0 + \underline{u}_1 e^{i\omega t}$	instantaneous total velocity vector, normalised by U
$\underline{u}_\infty$	free stream velocity vector
$\underline{u}_0$	steady perturbation velocity vector
$\underline{u}_1$	unsteady perturbation velocity vector
$\underline{\Gamma} = \underline{\Gamma}_0 + \underline{\Gamma}_1 e^{i\omega t} + \underline{r} e^{i\omega t} \times \underline{\Gamma}_0$	total circulation vector, normalised by U
$\underline{\Gamma}_0$	steady circulation vector
$\underline{\Gamma}_1$	unsteady circulation vector
$\omega_r = \frac{i\omega}{U}$	wave number

1. INTRODUCTION

The subsonic doublet lattice method (DLM) [1] has been the workhorse of aeroelastic analysis for several decades. Despite its widespread use, it is not suitable for the analysis of T-tail flutter in its basic form.

The essence of the T-tail problem is that the DLM only calculates the unsteady aerodynamic loads and generalised forces due to pitching and plunging of a lifting surface. This is acceptable for a conventional horizontal tail plane, however, for a T-tail the horizontal tail plane (HTP) sits on top of a flexible fin, and thus experiences significant rolling, yawing and spanwise in-plane motion, in addition to the usual pitching and plunging motion. Both in-plane loads and normal loads due to in-plane motion become important.

In addition to including in-plane motions and loads in the analysis, it is also necessary to consider the quadratic component of the natural modes. For example, in the case of a fin bending mode, the top of the fin moves along a circular arc. In the case of a fin torsion mode the fin actually shortens and the stabiliser moves normal to itself. Under these circumstances the steady load on the stabiliser contributes significantly to the unsteady generalised forces.

A further complication is that the incremental aerodynamic loads due to roll and yaw acting on the horizontal tail plane are dependent on the steady aerodynamic load.
In practical terms this complication adds another 'dimension' to the flight envelope that needs to be cleared for flutter - i.e. in addition to altitude, speed and aircraft configuration, the range in steady loading on the HTP also needs to be cleared for flutter. Estimating the range in steady loading on the HTP is a huge task in itself.

In the present study the unsteady boundary conditions as well as the calculation of unsteady forces were generalised to account for the in-plane loads as well as the normal loads due to in-plane motions. In addition, the steady load and the quadratic modeshape components were taken into account in the calculation of generalised forces. The T-tail extensions were implemented in a DLM with a surface panel body representation including a separated wake model. The same code is used to solve the steady flow field and the unsteady loads.

2. THEORY

The solution process for the T-tail DLM differs from that of the wing-body code only in that the more general boundary condition for body surface panels is also applied to lifting surfaces. The boundary condition is briefly stated and then the calculation of forces is addressed. The calculation of in-plane loads and of normal loads due to in-plane motion is based on the work of Queijo [2].

2.1 Lifting surface boundary condition

For the T-tail application the same boundary condition as for body panels is employed for lifting surface panels. The general form of the boundary condition is:

$$\dot{\underline{h}} \cdot \underline{n} = \underline{u} \cdot \underline{n} \tag{1}$$

or

$$\omega_r \underline{h} e^{i\omega t} \cdot \left(\underline{n}_0 + \underline{r} \times \underline{n}_0 e^{i\omega t} \right) = \left(\underline{u}_\infty + \underline{u}_0 + \underline{u}_1 e^{i\omega t} \right) \cdot \left(\underline{n}_0 + \underline{r} \times \underline{n}_0 e^{i\omega t} \right) \tag{2}$$

The steady boundary condition is simply:

$$\underline{u}_0 \cdot \underline{n}_0 = -\underline{u}_\infty \cdot \underline{n}_0 \tag{3}$$

Rigid body motion is assumed to uncouple the unsteady boundary condition from the steady disturbance flow. With this assumption, the unsteady boundary condition is:

$$\underline{u}_1 \cdot \underline{n}_0 = \omega_r \underline{h} \cdot \underline{n}_0 - \underline{u}_\infty \cdot \left(\underline{r} \times \underline{n}_0 \right) \tag{4}$$

The general form of the second factor in the second term takes account of yaw/dihedral coupling and the general form of the first term takes account of unsteady sideslip/dihedral coupling (note that $\omega_r \underline{h}$ may represent the unsteady sideslip velocity).

2.2 Calculation of forces for lifting surface panels

Although the downwash equation relates a pressure differential over a panel to the induced velocity, it is appropriate for T-tail configurations to calculate the forces as the cross product of the flow velocity and the circulation vector. Three vortex elements per box need to be considered: the quarter-chord bound vortex and the two chordwise-bound trailing vortices. The strength of the quarter-chord bound vortex is derived from the box pressure differential. The strength of the chordwise-bound vortices is given by the sum of the strengths of the upstream quarter-chord bound vortices.

The appropriate quarter-chord circulation vector, $\underline{\Gamma}$, is minus one half the box chord times the pressure coefficient differential (as determined by solving the downwash equation) times the vector from the doublet line inboard end to the outboard end.

$$\underline{F} = \underline{V} \times \underline{\Gamma} \tag{5}$$

where $\underline{F}$ is the total force, normalised by dynamic pressure, and $\underline{V}$ must be regarded as the relative flow velocity, normalised by the free stream velocity. The total circulation is given by

$$\underline{\Gamma} = \underline{\Gamma}_0 + \underline{\Gamma}_1 e^{i\omega t} + \underline{r} e^{i\omega t} \times \underline{\Gamma}_0 \tag{6}$$

The total relative velocity is given by

$$\underline{V} = \underline{u}_\infty + \underline{u}_0 + \underline{u}_1 e^{i\omega t} - \omega_r \underline{h} e^{i\omega t} \tag{7}$$

The induced velocity and modal displacement are those at the doublet line midpoint. The steady part of the total force is given by

$$\underline{F}_0 = (\underline{u}_\infty + \underline{u}_0) \times \underline{\Gamma}_0 \tag{8}$$

and the first harmonic of the total force is given by

$$\underline{F}_1 = (\underline{u}_\infty + \underline{u}_0) \times \underline{\Gamma}_1 + (\underline{u}_\infty + \underline{u}_0) \times (\underline{r} \times \underline{\Gamma}_0) + (\underline{u}_1 - \omega_r \underline{h}) \times \underline{\Gamma}_0 \tag{9}$$

The first term includes the normal force that is usually calculated by the DLM and is due to the unsteady circulation. $\underline{u}_0$ is usually neglected as it is small compared to $\underline{u}_\infty$.

The second term is due to the change in direction of the steady circulation vector. This accounts for both lateral load due to roll and rolling moment due to yaw (in the case of a swept HTP).

The third term includes the unsteady induced drag and the unsteady lift and drag due to the motion of the doublet line. It is acknowledged that this way of calculating induced drag is not physically correct but fortuitously provides a useful estimate.

2.3 Forces on chordwise bound vortices

The forces resulting from the interaction of spanwise flow with the chordwise bound vortices also need to be considered. In the vortex lattice method the trailing vortices, i.e. the chordwise bound vortices, have constant strength from one bound vortex to the next downstream bound vortex or to the wing trailing edge. In the present method these segments of the chordwise bound vortices are associated with the upstream aerodynamic box. The displacements of the vortex segment midpoints are calculated from the upstream box modal displacements, and the velocities at these points are taken to be the same as at the bound vortex midpoint except that the normal component is removed. In the case of an isolated flat wing the wing elements do not induce in-plane velocities in the plane of the wing. The gradients of the in-plane velocities are therefore small and it seems justified not to compute induced velocities at each trailing vortex segment midpoint.

In unsteady flow, the strength of the trailing vortices also vary in the chordwise direction due to the flow unsteadiness. This spatial variation is accompanied by a continuous sheet of vorticity being shed from the doublet line. This sheet of shed vorticity is however convected downstream by the flow and no force is generated from it. It is therefore only necessary to take account of the variation in the strength of the trailing vortices.

2.4 Calculation of forces for body panels

The original derivation for the surface panel body model did not consider the unsteady force resulting from the rotation of the steady force vector. The total force is given by

$$\underline{F} = -C_p \underline{n} \tag{10}$$

Note that the normal vector is not a unit vector, but has a length equal to the panel area, and that the normal vector has a steady and an unsteady component. The pressure coefficient is given by

$$C_p = C_p^0 + e^{i\omega t} C_p^1 \tag{11}$$

and the instantaneous normal vector by

$$\underline{n} = \underline{n}_0 + \underline{r} e^{i\omega t} \times \underline{n}_0 \tag{12}$$

The mean value of the force is

$$\underline{F}_0 = -C_p^0 \underline{n}_0 \tag{13}$$

And the first harmonic

$$\underline{F}_1 = -C_p^0 (\underline{r} \times \underline{n}_0) - C_p^1 \underline{n}_0 \tag{14}$$

The first term is the unsteady component due to the rotation of the steady force vector and the second term is due to the unsteady pressure on the panel. All the modal displacements and rotations are those at the panel centroid.

2.5 Calculation of generalised forces

The forces calculated as described above may lead to spurious generalised forces if a linear description of the modal displacement is used. Imagine a panel on an annular wing, generating a steady outward lift force and executing a circular arc motion about the axis of the annular wing. The rotation will give rise to a tangential force (due to the rotation of the force vector) as well as a tangential motion. The resulting generalised force (an unstable stiffness force) is, however, spurious and is only cancelled by the generalised force resulting from the steady lift force and the quadratic normal displacement.

The displacement of the doublet line midpoint in the case of a lifting surface panel or the panel centroid in the case of a body surface panel is given by

$$\underline{h} = \sum_{i=1}^{n} q_i \underline{h}_i^1 e^{i\omega t} + \sum_{i=1}^{n} q_i^2 \underline{h}_i^2 \left(e^{i\omega t}\right)^2 \tag{15}$$

The total force is given by

$$\underline{F} = \underline{F}_0 + \sum_{j=1}^{n} q_j \underline{F}_j e^{i\omega t} \tag{16}$$

The virtual work is defined as

$$\delta W = \sum_{i=1}^{n} \delta q_i Q_i = \sum_{i=1}^{n} \delta q_i \sum_{j=1}^{n} Q_{ij} q_j \tag{17}$$

The virtual work can also be derived from eqs. (15) and (16) as

$$\delta W = \delta \underline{h} \cdot \underline{F} = \sum_{i=1}^{n} \delta q_i \underline{h}_i^1 e^{i\omega t} \cdot \left(\underline{F}_0 + \sum_{j=1}^{n} q_j \underline{F}_j e^{i\omega t} \right) + \sum_{i=1}^{n} 2 q_i \delta q_i \underline{h}_i^2 \left(e^{i\omega t} \right)^2 \cdot \left(\underline{F}_0 + \sum_{j=1}^{n} q_j \underline{F}_j e^{i\omega t} \right) \tag{18}$$

Only terms containing $\left(e^{i\omega t}\right)^2$ need to be considered. The elements of the generalised force matrix are therefore defined by

$$\begin{aligned} Q_{ij} &= \underline{h}_i^1 \cdot \underline{F}_j, i \neq j \\ Q_{ii} &= \underline{h}_i^1 \cdot \underline{F}_i + 2\underline{h}_i^2 \cdot \underline{F}_0 \end{aligned} \tag{19}$$

The higher harmonic of the modal displacement needs to be entered by the user or some pre-processor. For bodies the modal displacement and rotation are entered on the reference axis. The transfer of rotation from the body axis to the body surface gives rise to quadratic displacements, which are added to the quadratic displacements on the axis.

For lifting surface panels the modal displacement and rotation are given at the spanwise and chordwise centre of the panel. The displacements at the collocation point and doublet line midpoint are calculated by the DLM, also taking account of the additional quadratic displacement.

2.6 The case for quadratic mode shapes: Π-tail example

The requirement for quadratic mode shapes is illustrated by the following example. Consider a finite planar wing with a mass of 5 kg, span 1 m and chord 0.25 m, suspended in space by two vertical supports of length 0.5 m, 0.5 m apart. The supports are stiff in the fore-aft sense and in the wing pitch sense, and are hinged at the top and bottom to allow lateral movement of the wing (Figs. 1 and 2). The wing is supported laterally by a linear spring with stifness constant 1 kN/m. This gives an air-off frequency of 2.25 Hz, ignoring gravtiy.

With the wing set at an angle of attack of 10° it would produce a lift force of 812.5 N (e=0.65) at a dynamic pressure of 5kPa. We know intuitively that the steady lift force would have a stiffening effect on the structure, similar to the effect of gravity on a pendulum. The steady lift force translates to a lateral spring stiffness of 1625 N/m . The frequency at this dynamic pressure would therfore be 3.65 Hz. Conversely, with the wing set at an angle of attack of –10°, the frequency would go to zero at a dynamic pressure of 3078 Pa.

To solve the frequency of the system using the present DLM, we note that for a (small) unit lateral displacement, the displacement of every point on the wing is given by

$$\begin{aligned} \underline{h}^1 &= (0,1,0) \\ \underline{h}^2 &= (0,0,-1) \end{aligned} \tag{20}$$

With this mode shape input the present DLM calculates a generalised force of -0.0326 m^2/Pa/°, irrespective of the reduced frequency. The frequency of the structure can be solved from the flutter equation as a function of dynamic pressure

$$1000 - 5\omega^2 = -0.0326 q\alpha$$

or (21)

$$\omega^2 = \frac{1000 + 0.0326 q\alpha}{5}$$

From this expression the frequency at 5 kPa dynamic pressure and 10° angle of attack can be solved as 3.65 Hz and the divergence dynamic pressure for –10° angle of attack as 3067 Pa.

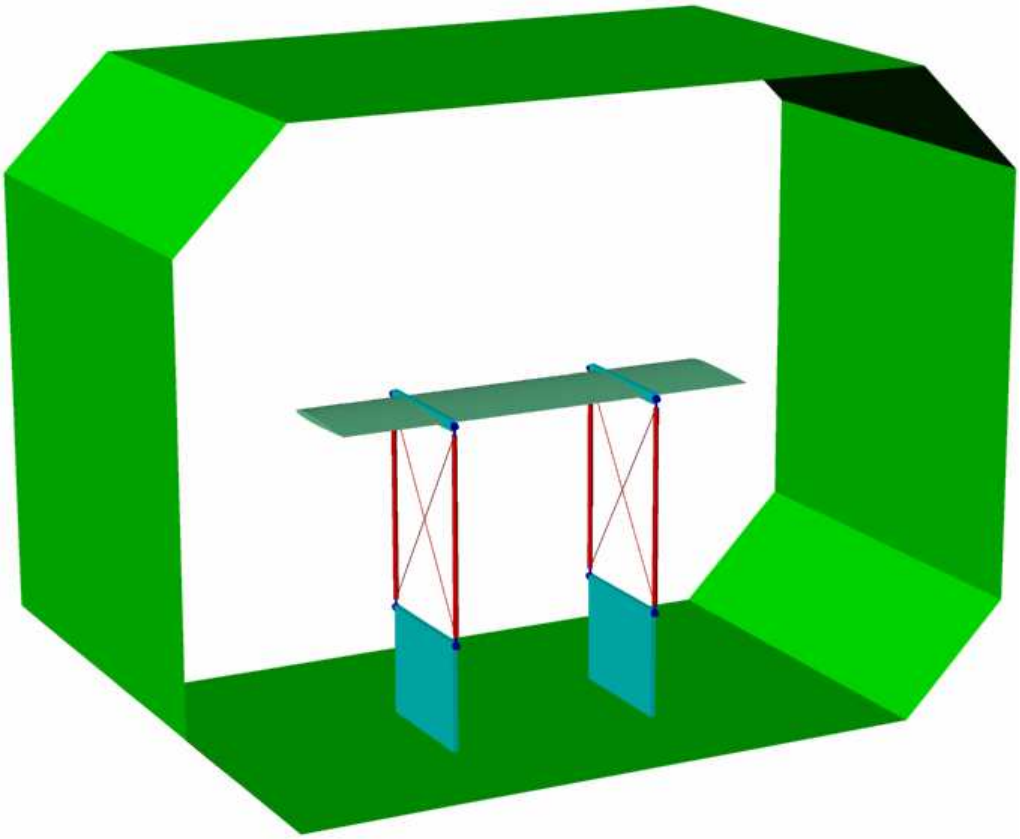

Figure 1: The hypothetical wing experiment as it might appear in a wind-tunnel (neutral position)

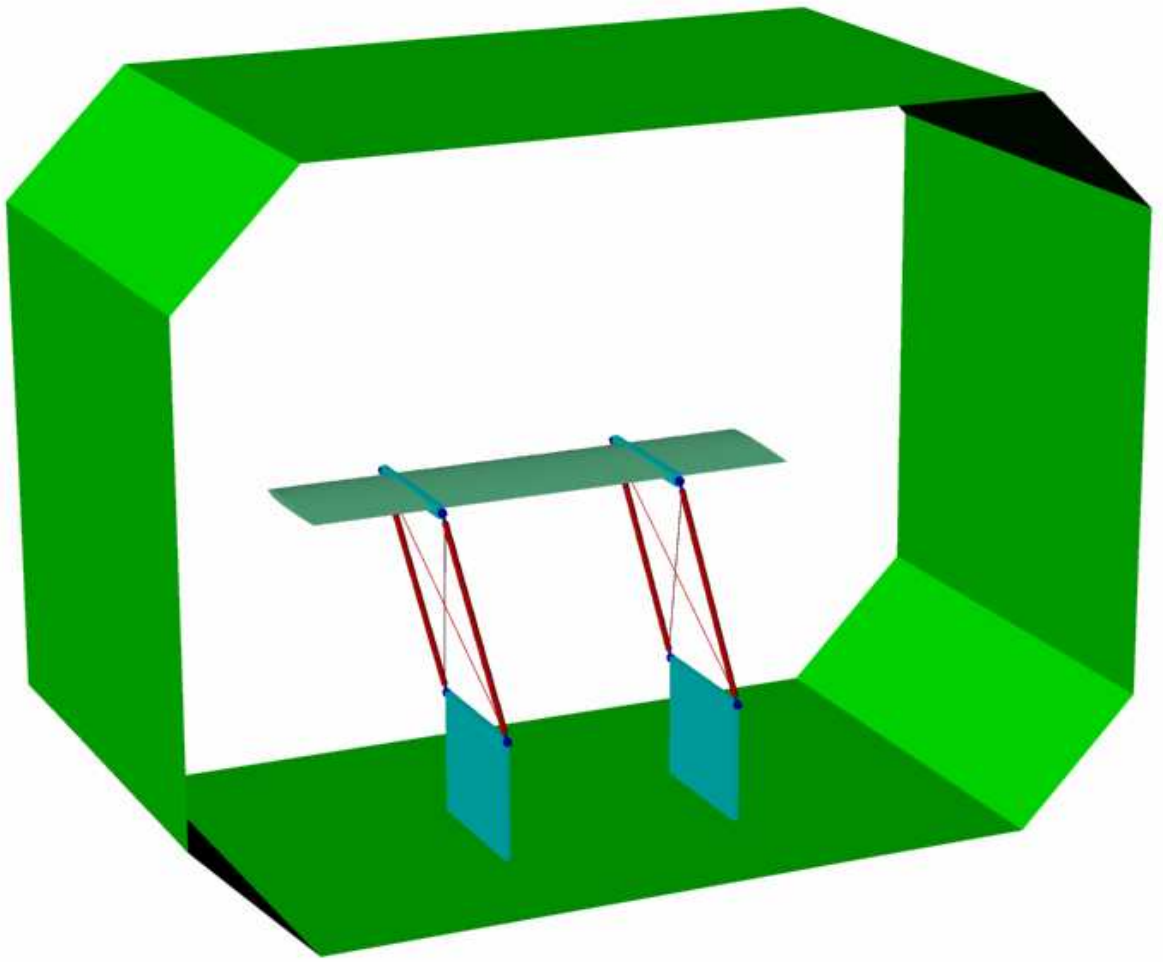

Figure 2: The hypothetical wing experiment as it might appear in a wind-tunnel (deflected)

2.7 Obtaining quadratic mode shapes

The question should be asked whether it is feasible to obtain quadratic mode shapes for general structures. This is possible and not too difficult using a sine-dwell ground vibration test system and inertial sensors (accelerometers), provided that the accelerometers measure down to zero frequency. The response due to the quadratic component occurs at twice the excitation frequency. Due to the rotation that the accelerometers may experience, one cannot simply take the response at twice the excitation frequency to be the quadratic component. The rotation of the accelerometer and the transverse acceleration produce a DC offset (a known problem in the use of accelerometers as angle of attack sensors in wind-tunnel models) as well as a response at twice the excitation frequency. The quadratic mode shape component can be solved from the DC offset and the response at twice the excitation frequency without knowing the actual rotation amplitude. In practice this requires testing at large amplitudes or using high precision instrumentation to obtain sensible results.

Quadratic displacements can also be readily obtained by post-processing of finite element analysis results. In the example of the simple T-tail shown in Fig. 3 below, a condition of zero in-plane stretching of the plate elements was enforced.

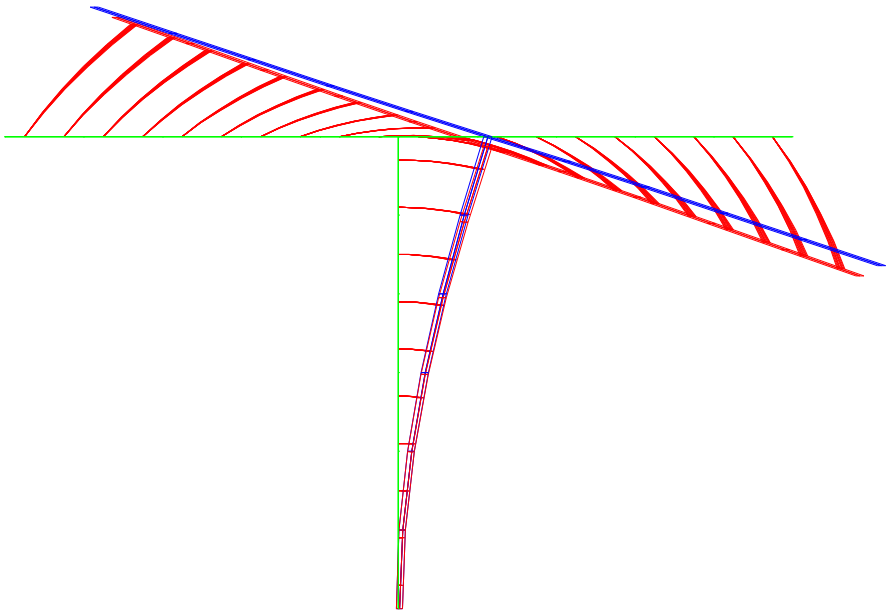

Figure 3: Quadratic mode shape of a simple T-tail: Green:undeflected, Blue: Linear deflection, Red: Quadratic deflection

3. CALCULATED RESULTS

Results from the present DLM were compared to Queijo's results for isolated wings executing different motions. The method was also applied to the flutter analysis of a simple T-tail flutter model.

3.1 Comparison with Queijo's results for isolated wings

Queijo gave extensive results for the following parameters for isolated wings without dihedral:

1. $\frac{C_{l_\beta}}{C_L}$ Rolling moment due to sideslip
2. $\frac{C_{l_r}}{C_L}$ Rolling moment due to yaw rate
3. C_{l_p} Roll damping
4. $\frac{C_{Y_p}}{C_L}$ Side force due to roll rate
5. $\frac{C_{n_p}}{C_L}$ Yawing moment due to roll rate

Note that of all these parameters, the standard DLM would only calculate roll damping. In the present DLM code it is possible to specify the steady angle of attack,

steady angle of sideslip and the 6 rigid body degrees of freedom as modes. The six degrees of freedom are

1. x-displacement
2. z-displacement
3. pitch
4. y-displacement
5. yaw
6. roll

The pitch and yaw rotations are specified around the origin, i.e. the root quarter-chord point. For some of Queijo's results the rotation centre is specified around the aerodynamic centre. It is therefore necessary to determine the aerodynamic centre from

$$x_{ac} = -\frac{Q_{30}}{Q_{20}} \tag{22}$$

where Q_{ij} is the generalised force corresponding to pressure mode j and displacement mode i. If j is zero, it indicates the steady (or mean) pressure distribution.

The estimates for Queijo's parameters in terms of the generalised forces calculated by the present method are given by

$$\frac{C_{l_\beta}}{C_L} = -\frac{Q_{60}/\beta}{bQ_{20}} = -\left.\frac{\mathrm{Re}(Q_{65})}{bQ_{20}}\right|_{k=0} = -\left.\frac{\mathrm{Im}(Q_{64})/|\omega_r|}{bQ_{20}}\right|_{k=0.01} \tag{23}$$

$$\frac{C_{l_r}}{C_L} = \frac{(\mathrm{Im}(Q_{65}) - x_{ac}\,\mathrm{Im}(Q_{64}))/|\omega_r|}{(b^2/2)Q_{20}} \tag{24}$$

$$C_{l_p} = \frac{\mathrm{Im}(Q_{66})/|\omega_r|}{S\,b^2/2} \tag{25}$$

$$\frac{C_{Y_p}}{C_L} = -\frac{\mathrm{Im}(Q_{46})/|\omega_r|}{(b/2)Q_{20}} \tag{26}$$

$$\frac{C_{n_p}}{C_L} = \frac{(\mathrm{Im}(Q_{56}) - x_{ac}\,\mathrm{Im}(Q_{46}))/|\omega_r|}{(b^2/2)Q_{20}} \tag{27}$$

The parameters rolling moment due to sideslip and rolling moment due to yaw rate compared well, except for the correction of 0.05 added to the rolling moment due to sideslip parameter. In the comparison below, this correction was omitted from Queijo's results.

The other parameters depend on the circulation distribution due to roll rate for which Queijo used a crude approximation. The comparison between the present results and Queijos' was therefore not very good. His approximation could however easily be incorporated into the present method in order to make a meaningful comparison. The circulation distribution due to roll rate was determined from the load distribution due

to angle of attack calculated using the present method by using Queijo's equation (4). With this approximation, the results for roll damping compare favourably.

The results for side force due to roll rate still did not compare well even with this approximation for the load distribution. The side force and yawing moment due to roll rate result from the interaction of the roll velocity and the steady (angle of attack) circulation. The present method uses the relative velocity of the air flow (which is the resultant of the free stream and the induced velocity at the doublet line midpoint) to determine the load on the doublet line, whereas Queijo neglected the induced velocity. In the comparison below, the induced velocity was also ignored in the present method.

The results below are for wings with a taper ratio of 0.5. Quejo's results were obtained by digitizing his plots of $\bar{y}^*$ and $\tilde{y}^*$, and using the digitized values in his expressions for the relevant parameters. The correction added to the rolling moment due to sideslip by Queijo was omitted. 64 spanwise strips on each semi-span were used in the present method.

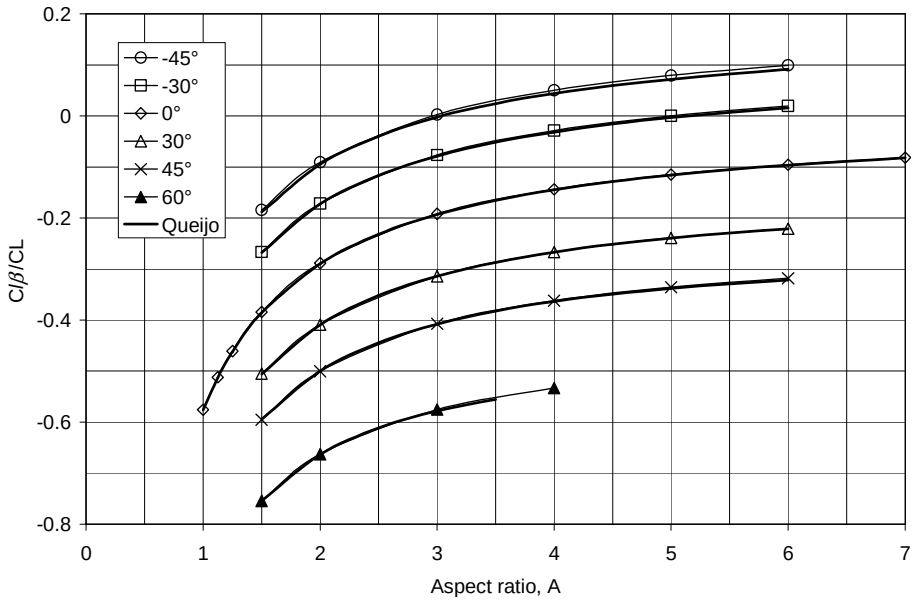

Figure 4: Rolling moment due to sideslip

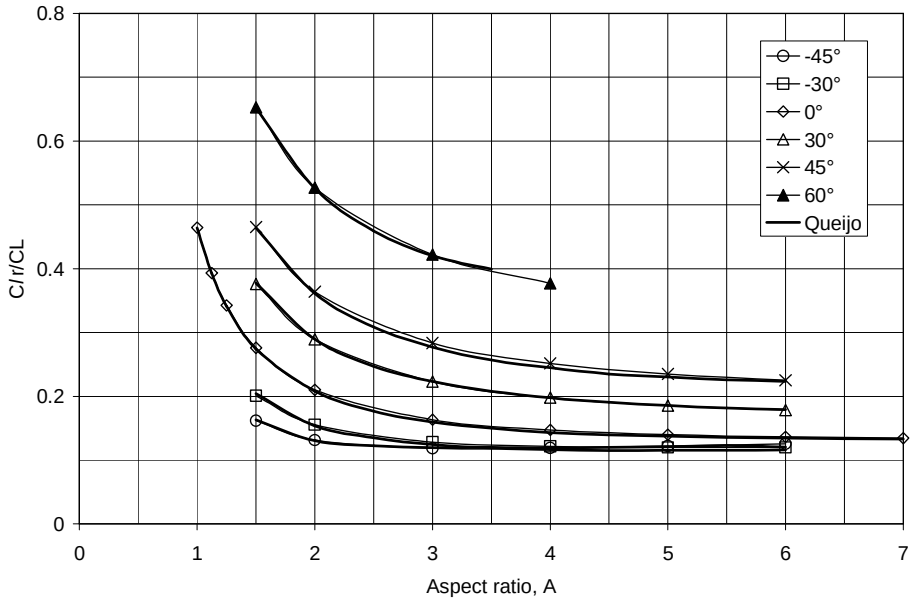

Figure 5: Rolling moment due to yaw rate

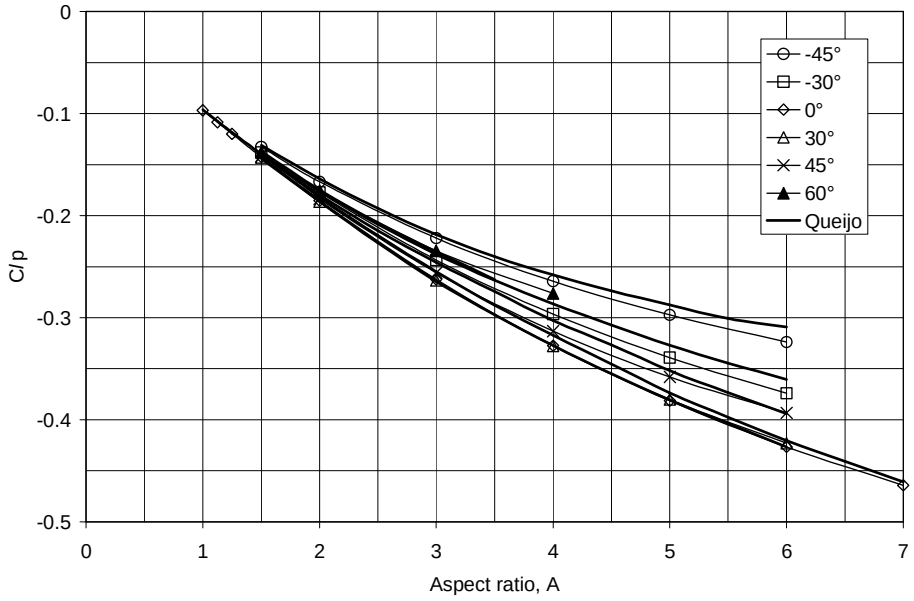

Figure 6: Roll damping

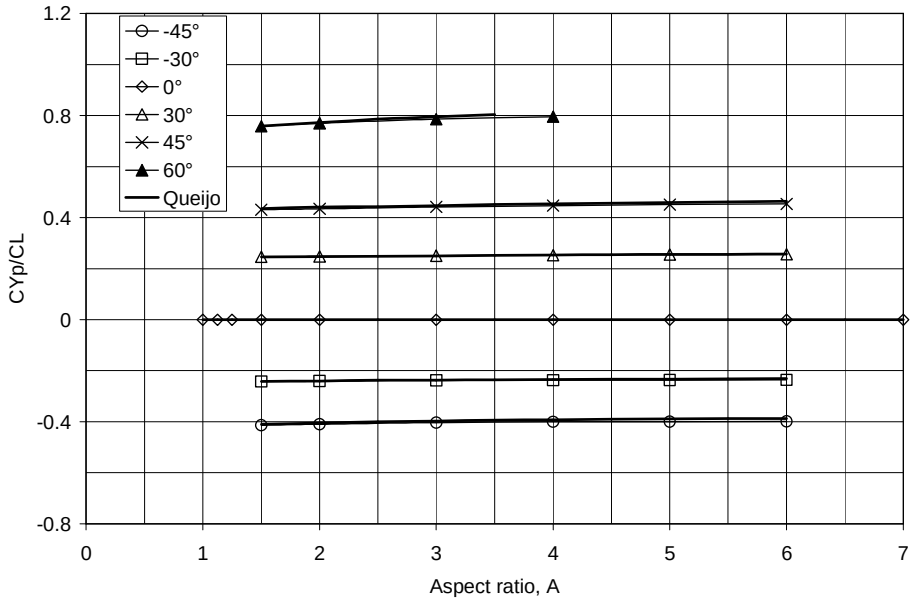

Figure 7: Side force due to roll rate

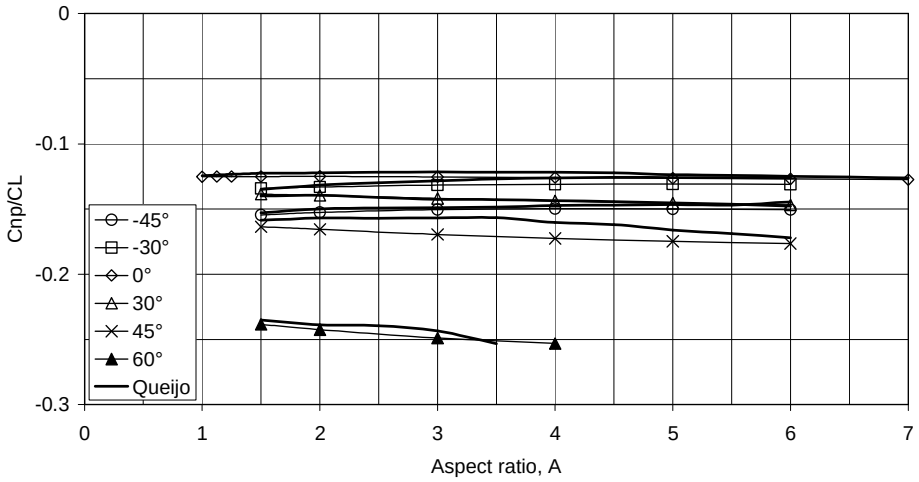

Figure 8: Yawing moment due to roll rate

3.2 Flutter analysis of a simple T-tail model

A simple T-tail flutter model was constructed from Aluminium plate and mounted on a base that allowed rotation about the vertical axis (Fig. 9). The flutter speed could be changed to suit the wind tunnel by changing the spring stiffness of the rotating base. The incidence of the HTP could be changed manually. The base also incorporated a plucking mechanism and a flutter amplitude limiter. The latter allowed the model to flutter safely and hence made it possible to obtain a precise flutter speed. The flutter speed graph below shows error bars on the experimental flutter speed from the highest speed at which flutter could not be induced, to the lowest speed at which flutter could be induced.

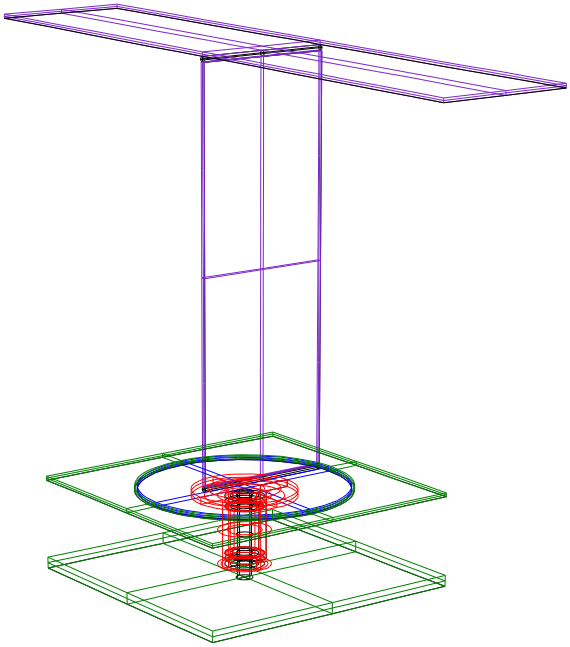

Figure 9: Simple T-tail flutter model construction

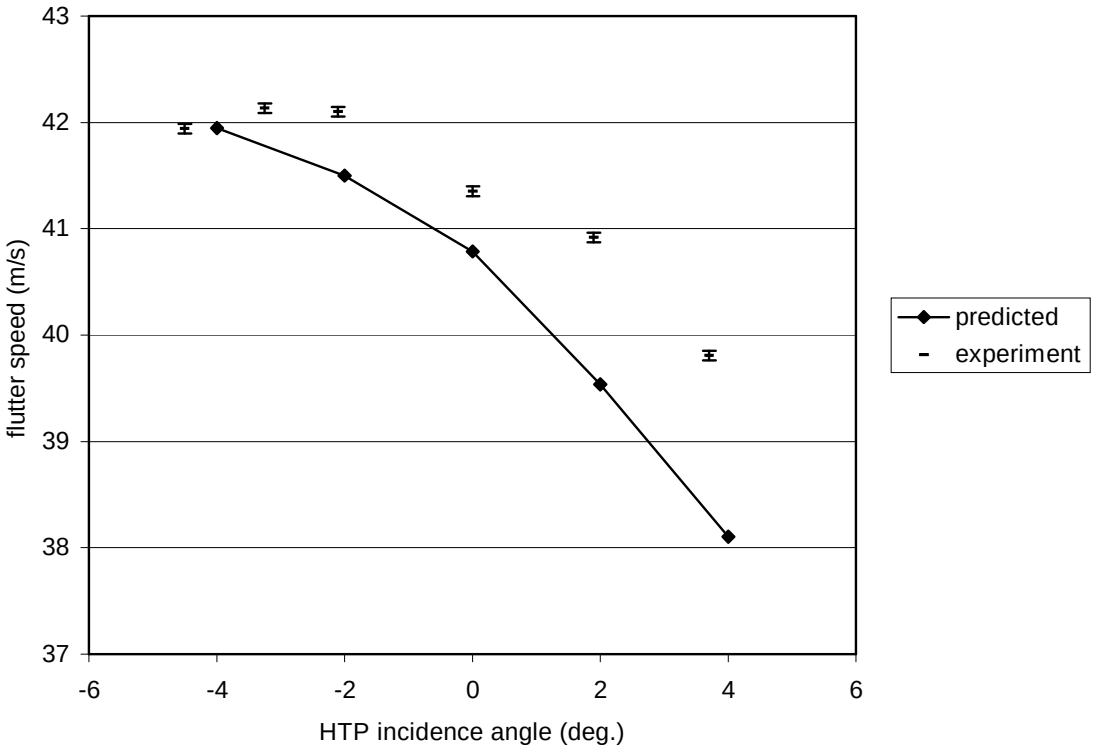

Figure 10: Flutter speed comparison for the simple T-tail model

MSC NASTRAN was used to determine the natural modes and post-processed to obtain the quadratic displacements. The present DLM was used to calculate generalised forces for a number of HTP incidence angles and the *p-k* formulation of the flutter equation was solved to obtain the flutter speed. The comparison between the calculated and measured flutter speeds is shown in Fig. 10. The agreement is reasonable.

4. ACKNOWLEDGEMENTS

The author wishes to thank Thomas Wilson of Airbus for providing him with a detailed explanation of the T-tail problem, which was used as the basis for the introduction of this paper.

The author also wishes to thank Dr Bill Rodden for making him aware of the work of Martin Queijo, which is really the enabling methodology for accounting for in-plane motion and loads.

5. CONCLUSIONS

The present DLM for T-tails models most of the phenomena that is necessary to predict T-tail flutter. Limited comparisons with experimental and published data to date were encouraging. Further experimental work to validate the method is in progress, including a larger model with a swept fin and stabiliser. The simple model will also be adapted to test the effect of dihedral. A transonic extension is not envisaged as fluid-structure coupled solutions are already viable for this application. Some aspects of the present work may be relevant to such solutions.

REFERENCES

[1] Rodden, W P, "*The development of the doublet-lattice method*", International Forum on Aeroelasticity and Structural Dynamics, Rome, June 1997

[2] Queijo, M. J. "Theory for computing span loads and stability derivatives due to sideslip, yawing, and rolling for wings in subsonic compressible flow," NASA TN D-4929, 1968